Article

Rh-Mediated Polymerization of Carbenes: Mechanism and Stereoregulation

Erica Jellema, Peter H. M. Budzelaar, Joost N. H. Reek, and Bas de Bruin

J. Am. Chem. Soc., **2007**, 129 (37), 11631-11641• DOI: 10.1021/ja073897+ • Publication Date (Web): 23 August 2007

J|A|C|S
ARTICLES
Published on Web 08/23/2007

Rh-Mediated Polymerization of Carbenes: Mechanism and Stereoregulation

Erica Jellema,[†] Peter H. M. Budzelaar,[‡] Joost N. H. Reek,[†] and Bas de Bruin*,[†]

Contribution from the Department of Homogeneous and Supramolecular Catalysis, Van't Hoff Institute for Molecular Sciences (HIMS), University of Amsterdam, Nieuwe Achtergracht 166, 1018 WV, Amsterdam, and Department of Chemistry, University of Manitoba, Winnipeg, MB, R3T 2N2, Canada

Received May 30, 2007; E-mail: bdebruin@science.uva.nl

Abstract: Ligand variation, kinetic investigations, and computational studies have been used to elucidate the mechanism of rhodium-catalyzed diazoalkane polymerization. Variations in the "*N,O*" donor part of the catalyst precursors (diene)Rh^{I}(*N,O*) result in different activities but virtually identical molecular weights, indicating that this part of the precursor is lost on forming the active species. In contrast, variation of the diene has a major effect on the nature of the polymer produced, indicating that the diene remains bound during polymerization. Kinetic studies indicate that only a small fraction of the Rh (1−5%) is involved in polymerization catalysis; the linear relation between polymer yield and M_w suggests that the chains terminate slowly and chain transfer is not observed (near living character). Oligomers and fumarate/maleate byproducts are most likely formed from other "active" species. Calculations support a chain propagation mechanism involving diazoalkane coordination at the carbon atom, N_2 elimination to form a carbene complex, and carbene migratory insertion into the growing alkyl chain. N_2 elimination is calculated to be the rate-limiting step. On the basis of a comparison of NMR data with those of known oligomer fragments, the stereochemistry of the new polymer is tentatively assigned as syndiotactic. The observed syndiospecificity is attributed to chain-end control on the rate of N_2 elimination from diastereomeric diazoalkane complexes and/or on the migratory insertion step itself.

Introduction

Metal-catalyzed (co)polymerization of functionalized olefins can be considered as the "holy grail" of polymerization catalysis.[1,2] It would not only afford access to new polymers with controlled monomer sequences, but would also allow precise tuning of stereochemistry through ligand variation. However, (co)polymerizing such monomers is not easy, because functional groups compete with the double bond for coordination to the transition metal (both before and after insertion) and also facilitate various types of side reactions that can lead to catalyst deactivation. Late transition metals tend to be less sensitive to both issues than early transition metals, and significant progress has been made in particular with Ni and Pd catalysts.[2] Nevertheless, this is by no means a solved problem.

Group transfer polymerization (GTP) is a convenient way to prepare acrylate and methacrylate polymers with narrow molecular weight distributions.[3] However, as is the case with radical (ATRP) and anionic polymerization, GTP methods give, at best, poor control over the polymer stereoproperties.[4]

One alternative route to the formation of highly functionalized polymers would be through polymerization of (substituted) diazoalkanes. Whereas unsubstituted diazoalkanes are inherently unstable, derivatives bearing electron-withdrawing substituents (such as diazoacetates, N_2CHCO_2R) are reasonably stable, safe[5] (even in large scale/industrial synthesis), easy to prepare, cheap, and therefore extensively used as carbene precursors in organic synthesis. In the presence of transition metals they generally convert to reactive carbene complexes, which can undergo dimerization (to form olefins), carbene transfer to olefins (cyclopropanation), and insertion into O−H, N−H and C−H bonds.[6] These reactions are most often mediated by mononuclear platinum, copper, and ruthenium catalysts, or dinuclear Rh(II)−acetates. They allow efficient and often

[†] University of Amsterdam.
[‡] University of Manitoba.

(1) Tullo, A. H. *Chem. Eng. News* **2001**, *79*(43), 35−36.
(2) (a) Williams, B. S.; Leatherman, M. D.; White, P. S.; Brookhart, M. *J. Am. Chem. Soc.* **2005**, *127*, 5132−5146. (b) Ittel, S. D.; Johnson, L. K.; Brookhart, M. *Chem. Rev.* **2000**, *100*, 1169. (c) Gibson, V. C.; Spitzmesser, S. K. *Chem. Rev.* **2003**, *103*, 283 and references therein.
(3) (a) Webster, O. W. *Science* **1991**, *251*, 887. (b) Webster, O. W. *J. Polymer Sci. A* **2000**, *38*, 2855−2860. (c) Webster, O. W. *Adv. Polymer Sci.* **2004**, *167*, 1−34.
(4) (a) Ute, K.; Ohnuma, H.; Shimizu, I.; Kitayama, T. *Polymer. J.* **2006**, *38*, 999−1003. (b) Ute, K.; Tarao, T.; Hongo, S.; Ohnuma, H.; Hatada, K.; Kitayama, T. *Polymer. J.* **1999**, *31*, 177−183. (c) Banerjee, K. G.; Hogen-Esch, T. E. *Polymer Prepr. (Am. Chem. Soc., Div. Polym. Chem.)***1987**, *28*, 320.
(5) (a) Clarck, J. D.; Shah, A. S.; Peterson, J. C. *Thermochim. Acta* **2002**, *392*−*392*, 177−186. (b) Clarck, J. D.; Shah, A. S.; Peterson, J. C.; Patelis, L.; Kersten, R. J. A.; Heemskerk, A. H. *Thermochim. Acta* **2002**, *386*, 73−79. (c) Clarck, J. D.; Shah, A. S.; Peterson, J. C.; Patelis, L.; Kersten, R. J. A.; Heemskerk, A. H.; Grogan, M.; Camden, S. *Thermochim. Acta* **2002**, *386*, 65−72. (d) Clarck, J. D.; Heise, J. D.; Shah, A. S.; Peterson, J. C.; Chou, S. K.; Levine, J.; Karakas, A. M.; Ma, Y.; Ng, K.-Y.; Patelis, L.; Springer, J. R.; Stano, D. R.; Wettach, R. H.; Dutra, G. A. *Org. Process Res. Dev.* **2004**, *8*, 176−185.
(6) (a) Merlic, C. A.; Zechman, A. L. *Synthesis* **2003**, 1137. (b) Ye, T.; McKervey, A. *Chem. Rev.* **1994**, *94*, 1092. (c) Maas, G. *Chem. Soc. Rev.* **2004**, *33*, 183.

Scheme 1. Formation of High-Molecular Weight Stereoregular Polymers by Rh-Mediated Polymerization of "Carbenes" Formed from EDA

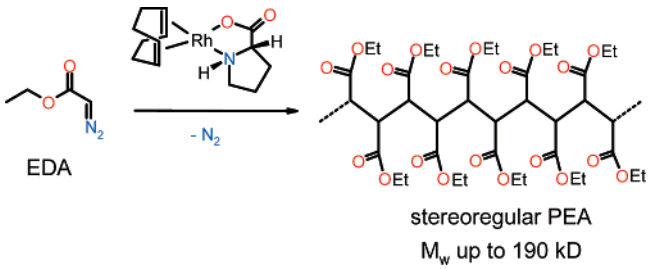

stereoselective conversion of the coordinated carbene to more or less sophisticated products.[6]

Carbene insertion into a transition metal−alkyl bond, which could lead to interesting functionalized polymers, is a far less common reaction.[7] There are a few reports describing BH_3-, Cu-, and Pd-mediated oligomerization of α-carbonyl stabilized "carbenes" formed from diazocarbonyl compounds, producing *atactic* low-molecular mass *oligomers*, with an average degree of polymerization ranging from a few up to ca. 100.[8−10] These materials are notable because they carry a polar functionality (amenable to further transformations) at *each* main-chain carbon atom. The only other route to such compounds has been through free-radical polymerization of dialkyl maleates or fumarates,[11] with no control over the resultant polymer stereochemistry.

We recently reported that a family of Rh(diolefin) complexes bearing nontraditional "hard" *N,O*-type ligands is able to polymerize carbenes formed from diazoacetates to yield stereoregular ester-functionalized polymethylenes with a high molecular mass.[12] In particular, the use of the amino-acid L-proline as a ligand for rhodium proved to give quite active and selective catalysts for the polymerization of carbonyl-substituted methylene carbenes (see Scheme 1). Polymers with molecular weights up to 190000 (M_w) were obtained as solid materials with interesting material properties. To date, there are no other catalysts that produce high-molecular mass or stereoregular polymethylenes with functional sidegroups. In the present paper, we assign the stereochemistry of the new polymer as *syndiotactic* on the basis of comparison of NMR data with those of reported oligomer fragments.[13] We also use ligand variation and DFT calculations to shed some light on the nature of the catalytically active species. We first focused on understanding the chain propagation mechanism to provide a rationale for the formation of *stereoregular* polymers. Investigations aiming at understanding initiation and termination pathways are ongoing and will be presented in another paper.

Scheme 2. Synthesis of Catalyst Precursors **1**−**7**

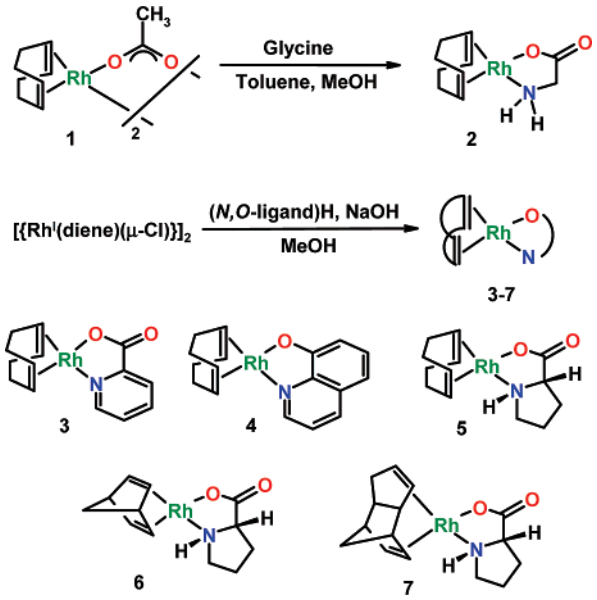

Results and Discussion

Catalyst Precursors. Previously, we reported that [(*N,O*-ligand)Rh^{I}(cod)] complexes are catalyst precursors for the polymerization of carbenes from alkyl diazoacetates.[12] In the search for the nature of the active species we focused on variation of both the *N,O*- and the diene-ligand of the [(*N,O*-ligand)Rh^{I}(diene)] species. The previously reported catalyst precursors, **3**−**5**,[12] and the new complexes **2**, **6**, and **7** used for the polymerization of carbenes formed from ethyl diazoacetate (EDA) are depicted in Scheme 2. Complexes **2**, **6**, and **7** were prepared according to the reactions shown (Scheme 2).

Similar to the previously reported complexes **3**−**5**, the complexes **2** and **6** reveal expected and uncomplicated NMR spectra, showing the presence of only a single isomer in solution. The new [(L-prolinate)Rh^{I}(*endo*-dicyclopentadiene)] complex **7** shows more complicated ^{1}H and ^{13}C NMR spectra due to the presence of four isomers. Reaction of enantiomerically pure L-proline (*S*-proline) with racemic [{(dcp)Rh(μ-Cl)}$_2$] in a 2:1 ratio is expected to result in formation of two diastereoisomeric [(L-prolinate)Rh^{I}(dcp)] species **7a** and **7b** in a 1:1 ratio. The NMR spectra clearly reveal the presence of four isomeric [(L-prolinate)Rh^{I}(dcp)] species, two by two (**7a** with **7a′** and **7b** with **7b′**) species in dynamic equilibrium with each other according to EXSY spectroscopy (see Figure 1). The species are present in different ratios (**7a**:**7a′**:**7b**:**7b′** = 1:0.9:1.2:0.6), but as expected the sum **7a** + **7a′** equals the sum **7b** + **7b′**. The spectroscopic difference between these species is most pronounced for the olefinic signals, both in ^{1}H NMR and in ^{13}C NMR. The olefinic signals f and g (see Figure 1) of the isomers **7a** and **7b** are substantially upfield shifted relative to those of **7a′** and **7b′**, whereas the a/b olefinic signals shift downfield (see Table 1). This clearly points to the presence of *cis*/*trans* isomers, with **7a** and **7b** having the more symmetrical f/g olefin *trans* to the anionic *O*-donor and **7a′** and **7b′** having the least symmetrical olefin a/b *trans* to this donor. Stronger metal-to-olefin π-back-donation to the olefin *trans* to the (π-donating) prolinate *O*-donor explains the observed upfield shifts of the different olefin signals.

(7) (a) Greenman, K. L.; Carter, D. S.; Van Vranken, D. L. *Tetrahedron* **2001**, 5219−5225. (b) Greenman, K. L.; Van Vranken, D. L. *Tetrahedron* **2005**, 6438.
(8) Bai, J.; Burke, L. D.; Shea, K. J. *J. Am. Chem. Soc.* **2007**, *129*, 4981−4991 and references therein.
(9) Liu, L.; Song, Y.; Li, H. *Polym. Int.* **2002**, *51*, 1047.
(10) (a) Ihara, E.; Haida, N.; Iio, M.; Inoue, K. *Macromolecules* **2003**, *36*, 36. (b) Ihara, E.; Fujioka, M.; Haida, N.; Itoh, T.; Inoue, K. *Macromolecules* **2005**, *38*, 2101. (c) Ihara, E.; Kida, M.; Fujioka, M.; Haida, N.; Itoh, T.; Inoue, K. *J. Polym. Sci., Part A: Polym. Chem.* **2007**, *45*, 1536−1545.
(11) Toyoda, N.; Yoshida, M.; Otsu, T. *Polym. J.* **1983**, *15*, 255.
(12) Hetterscheid, D. G. H.; Hendriksen, C.; Dzik, W. I.; Smits, J. M. M.; van Eck, E. R. H.; Rowan, A. E.; Busico, V.; Vacatello, M.; Van Axel Castelli, V.; Segre, A.; Jellema, E.; Bloemberg, T. G.; de Bruin, B. *J. Am. Chem. Soc.* **2006**, *128*, 9746−9752.
(13) Yoshioka, M.; Matsumoto, A.; Otsu, T.; Ando, I. *Polymer* **1991**, *32/15*, 2741−2746.

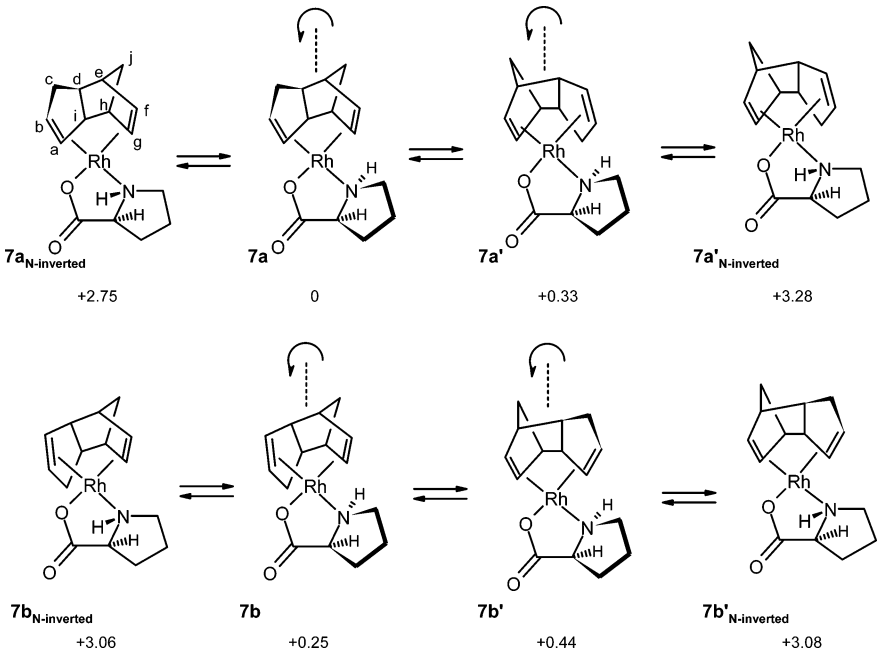

Figure 1. Relative energies of the DFT optimized (Turbomole, b3-lyp, TZVP) geometries of diastereoisomers **7a** and **7b**, each consisting of four possible geometrical isomers as a result of cis−trans isomerism and pyramidal inversion at nitrogen (in kcal/mol, not corrected for ZPE or thermal effects).

Table 1. Chemical Shift Values of the Olefinic NMR Signals of **7a**, **7a′**, **7b**, and **7b**[a,b]

	^{1}H δ (ppm)				^{13}C δ (ppm)			
	7a	**7a′**	**7b**	**7b′**	**7a**	**7a′**	**7b**	**7b′**
a	4.81	4.04	4.92	4.52	87.59	78.48	87.08	78.48
b	4.92	4.04	4.98	4.04	85.22	73.59	84.18	73.22
f	3.81	4.67	4.04	4.70	64.84	75.94	65.78	75.14
g	5.50	6.39	5.18	6.20	89.59	102.28	90.52	101.82

[a] Measured in $CDCl_3$ at 298 K (^{1}H: 500 MHz and ^{13}C: 125 MHz). [b] For labeling, see Figure 1.

In good agreement with the experimentally derived ratios, DFT calculations reveal that the species **7a′** and **7b′** lie about +0.33 and +0.19 kcal/mol higher in energy than **7a** and **7b**, respectively (Figure 1).

Coordination of the prolinate nitrogen makes this donor enantiotopic, and in principle both *R* and *S* configurations are possible for this atom through pyramidal inversion. In a previous report we published the X-ray structure of the [(L-prolinate)-Rh^I(cod)] analogue, revealing an *S* configuration of the *N*-donor (and no other isomers were observed with NMR spectroscopy).[12] We expected **7a** and **7b** to behave in a similar way, and indeed the relative energies (DFT calculations) of the species having a nitrogen *R* configuration (**7a**$_{\mathbf{N-Inverted}}$, **7a′**$_{\mathbf{N-inverted}}$, **7b**$_{\mathbf{N-Inverted}}$, and **7b′**$_{\mathbf{N-inverted}}$) are about 3 kcal/mol higher compared to the respective species having a nitrogen *S* configuration (Figure 1). In line with this, these N-inverted species were not detected by NMR spectroscopy.

Carbene Polymerization Reactions. Polymerization reactions were carried out by addition of 50 equiv of EDA to a solution of the catalyst precursor in chloroform at room temperature. After 14 h the solvent was evaporated, and the polymer (poly(ethyl 2-ylidene-acetate), PEA) was isolated and washed with methanol. For all catalysts except **6**, ^{1}H NMR spectroscopy indicated complete conversion of EDA after 14 h.

The polymers and oligomers were analyzed by size exclusion chromatography (SEC) calibrated with polystyrene samples. These molecular weights and weight distributions, therefore, deviate slightly from the previously reported data, which were calibrated with MALLS.[12]

If we focus on the formation of well-defined stereoregular PEA, it is clear that the use of the Rh(cod) catalyst precursors **1**−**5** with different *O*,*O*- and *N*,*O*-ligands (chiral and non-chiral) produces virtually identical polymers with comparable molecular weights and weight distributions, albeit in different yields (entries 1−5). These results suggest that the *O*,*O*- or *N*,*O*-ligands might be involved in the initiation of the polymerization but are unlikely to act as stabilizing ligands to Rh during the propagation steps. In contrast, varying the diene ligand of the [(L-prolinate)Rh^I(diene)] catalyst precursors **5**−**7** leads to polymers with very different molecular weights and weight distributions (entries 5−7). Most remarkably, the Rh^I complex with the dicyclopentadiene (dcp) ligand (**7**) produces substantially *higher*-molecular weight polymers (M_w = 540 kD) with a much *narrower* molecular weight distribution (M_w/M_n = 2.0) compared to the previously reported cod analogue **5** (M_w = 150 kD, M_w/M_n = 3.6) under otherwise identical reaction conditions (Table 2). These data clearly point to the involvement of Rh-(diene) species in the chain propagation.[14] Since high-molecular weight polymers are obtained while using only 50 equiv of EDA, only a few percent of the catalyst precursor can be active in the polymerization reaction (**5**: ∼3%, **7**: ∼1%). These low initiation efficiencies do not exclude the possibility of Rh adventitious impurities playing a role in the catalytic reaction. However, different batches of the Rh(diene) catalysts, prepared from different Rh sources, give rise to identical results in the catalytic carbene polymerization. Using repeatedly recrystallized batches of catalyst precursor **5** and freshly distilled EDA and

(14) Ancillary (chiral) diene ligands have also been observed to support the active species in Rh-mediated polymerization of phenylacetylene and asymmetric 1,4-additions to α,β-unsaturated ketones: (a) Saeed, I.; Shiotsuki, M.; Masuda, T. *Macromolecules* **2006**, *39*, 8977−8981. (b) Otomaru, Y.; Kina, A.; Shitani, R.; Hayashi, T. *Tetrahedron: Asymmetry* **2005**, *16*, 1673−1679. (c) Kina, A.; Ueyama, K.; Hayashi, T. *Org. Lett.* **2005**, *7*, 5889−5892.

Table 2. Polymerization of Carbenes Formed from EDA with Catalysts **1**−**7**[a]

catalyst	diene	PEA %[b]	M_w (kD)[b,c]	M_w/M_n[b,c]	oligomer %[c,d]	M_w (kD)[c,d]	M_w/M_n[c,d]	maleate/ fumarate %[e]
1	cod	15	150	3.7	57	1.1	2.6	28
2	cod	30	150	3.4	37	1.0	3.6	33
3	cod	11	130	3.7	nd	nd	nd	nd
4	cod	11	140	3.7	nd	nd	nd	nd
5	**cod**	50	**150**	**3.6**	30	1.2	2.6	20
6	**nbd**	5[f]	**350**	**15.4**[g]	53[f]	1.4	3.6	7[f]
7	**dcp**	30	**540**	**2.0**	38	1.1	4.5	32

[a] Conditions: 0.04 mmol catalyst; 2 mmol EDA, 5 mL chloroform (solvent), room temperature, reaction time: 14 h. [b] Isolated by precipitation and washing with methanol. [c] SEC analysis calibrated against polystyrene samples. [d] Combined methanol soluble fractions after evaporation of the solvent. [e] Estimated yield; part of the combined diethyl maleate and fumarate fraction is lost during workup of the polymer and oligomer fractions, using a vacuum pump. [f] ~35% EDA recovered. [g] Bimodal distribution.

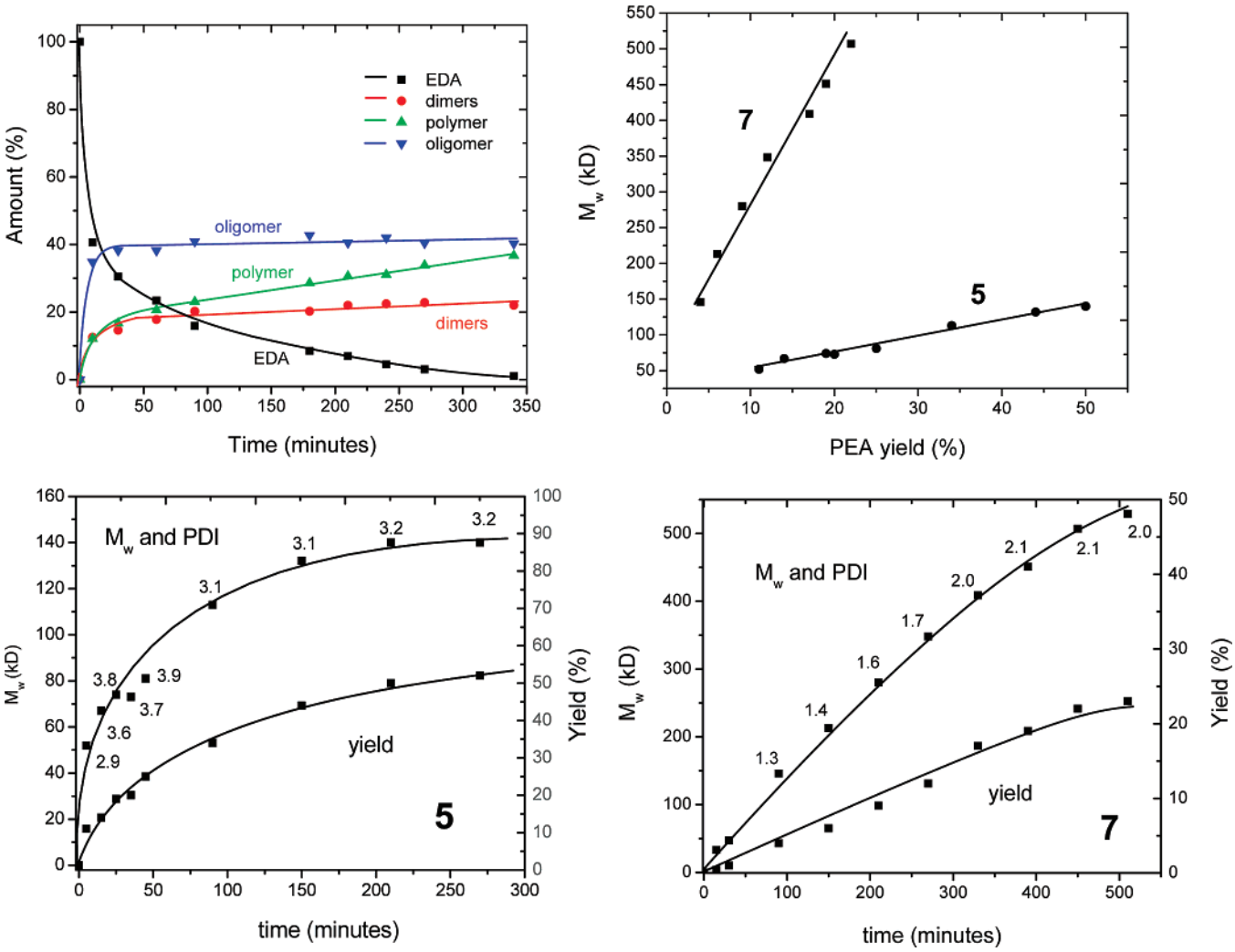

Figure 2. Time−product profiles for carbene polymerization reactions. (Top Left) Development of the product distribution in time using catalyst precursor **5**. (Top Right): Correlation between the molecular weights of the polymer (M_w in kD) and obtained PEA yields (%) for catalyst precursors **5** and **7**. (Bottom) Development of the polymer molecular weights and yields in time using catalyst precursors **5** and **7**. The numbers represent the obtained PDI values (M_w/M_n) for each SEC sample.

solvent has no beneficial effect on the catalytic performance at all, and deliberately adding water and/or introducing oxygen has only a minor negative influence on the obtained polymer yields. Furthermore, it is relevant to note that for Rh(diene)-mediated polymerization of phenylacetylene inefficient initiation (<5%) is quite commonly observed, with ligand modifications having a substantial beneficial effect on the initiation efficiencies (reaching up to 100% as recently reported by Masuda et al.).[15]

Note that the behavior of **7** points to generation of a single-site active catalyst, while the spectroscopic data of the precata-

(15) Saeed, I.; Shiotsuki, M.; Masuda, T. *Macromolecules* **2006**, *39*, 8567−8573.

lyst clearly revealed the presence of four different isomeric species in solution. These data further support the idea of prolinate dissociation upon generation of the catalytically active species.

For the reactions with complexes **1**, **2**, **5**, **6**, and **7** we also analyzed the methanol soluble fractions left after workup and washing the PEA with methanol. From this it became clear that besides the previous reported (methanol insoluble) *stereoregular polymer* and small amounts of diethyl maleate and fumarate, the reactions also produce varying amounts of *oligomers* with a number degree of polymerization of only about 11−20 "carbene" units. The extremely broad NMR spectra of these oligomers (see Figure S1, Supporting Information) point to a poorly defined structure, which is not at all related to the well-defined structure of the stereoregular polymer. It is clear that all of the applied catalyst precursors produce the same poorly defined oligomers (identical NMR spectra and identical M_w and M_w/M_n within experimental errors, see Table 2). It is thus unlikely that the oligomerization process involves the same catalytically active species responsible for the polymerization event.

We monitored the polymerization reaction catalyzed by cod complex **5** in time by ^{1}H NMR spectroscopy. As shown in Figure 2 (top left), the applied conditions lead to rather fast EDA consumption in the beginning of the reaction, with production of most of the byproducts. Within 1 h most (>75%) of the EDA has been consumed, and the reaction mixture consists of ∼38% oligomers, ∼15% diethyl maleate and fumarate dimers (combined), and only ∼21% of polymer. After 1 h the total amount of diethyl maleate/fumarate and oligomer byproducts hardly increases further (within experimental errors), and consumption of the remaining EDA almost exclusively leads to stereoregular PEA (Figure 2, top left). The final product distribution determined with NMR spectroscopy deviates only slightly from the distribution of isolated products (Table 2), which is reasonable considering substantial experimental and integration errors associated with ^{1}H NMR integrations.[16]

SEC analysis of stereoregular PEA samples obtained after varying reaction times yields further information. With catalyst precursor **5** (Figure 2, bottom left), the polydispersity values (PDI) of the obtained polymers is quite large initially (ca. 3.0), increases further in the first hour of the reaction to about 4.0, and then slowly decreases to a limiting value of ca. 3.0. Formation of PEA using catalyst precursor **7** (Figure 2, bottom right) is slower. The molecular weight distribution is quite narrow initially (PDI ≈1.3) but broadens over time (to a PDI of ca. 2.0).

The nearly linear correlation between the molecular weight and yield for polymer samples obtained with both catalyst precursors **5** and **7** (Figure 2, top right) is an indication for a chain-growth mechanism proceeding without detectable chain transfer (near-living character). The gradually broader molecular weight distribution of polymer samples obtained with catalyst precursor **7** in time points to slow termination of the chain-propagating species. This is happening under conditions of monomer depletion, which potentially limits the molecular weight. However, using much more EDA (100 equiv) leads to much lower overall yields (with nonconverted EDA being recovered after the reaction) and does not lead to an increase in the molecular weight of the obtained polymer. This clearly suggests that the active species deactivates in time, even in the presence of enough monomer. Further investigations in which different concentrations of EDA are slowly added in time may lead to further process optimization, but future efforts aiming at finding more efficient ways to initiate the polymerization are likely more rewarding.

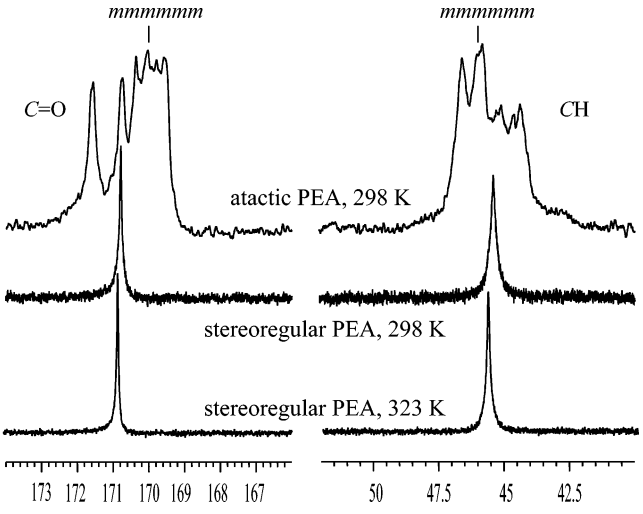

Figure 3. (Top) ^{13}C NMR spectrum ($CDCl_3$, 75 MHz, 298 K) of *atactic* PEA prepared by radical polymerization of diethylfumarate,[12] with assignment of the *mmmmmm* heptad microstructure signals according to ref 13. (Middle) ($CDCl_3$, 125 MHz, 298 K) and (Bottom) ($CDCl_3$, 125 MHz, 323 K): ^{13}C NMR spectra of *stereoregular* PEA prepared with rhodium catalyst **7** (Table 2, entry 7).

The capricious behavior of the polymer PDI values in time for samples obtained with catalyst precursor **5** is not so easily understood in terms of a single-site catalyst, and perhaps **5** generates more than one species active in the carbene polymerization process. Somewhat higher-molecular weight PEA (205 kD) is attainable with catalyst precursor **5** upon addition of an additional amount of EDA (25% of the initial amount) after 1 h. This leads to an overall PEA yield of only 45% (60% is expected with full conversion of, at that point, nonconverted plus additional EDA to PEA), again suggesting that, even in the presence of enough monomer, termination processes stop the polymerization reaction before complete EDA conversion.[17]

Assignment of Stereochemistry. The polymers obtained with [(L-prolinate)Rh^I(cod)] are highly stereoregular, as shown by detailed NMR spectroscopy studies in our previous paper.[12] PEA samples obtained with other Rh(diene) species give rise to virtually identical NMR spectra and must thus have the same microstructures (either all isotactic or all syndiotactic). A detailed analysis by Otsu et al. of ^{13}C NMR data of atactic poly(dialkyl fumarate)s with varying isoactic enrichments (depending on the radical polymerization method) has allowed assignments of the carbonyl and methine ^{13}C NMR signals to the heptad microstructures mmmmmm, mmmmmr, mmmmrm, rmmmrm, mmmrmm, mmmrmr, mrmrmm, and mrmrmr.[13] Unfortunately,

(16) Especially the oligomer contents in Figure 2 (left) are not highly reliable. The oligomer backbone *CH*(COOEt) protons are very broad, hardly detectable, and overlap with other signals, and are thus not suitable for direct ^{1}H NMR integration. The relative oligomer contents are therefore estimated by subtracting the expected integral contributions of EDA, PEA, and diethyl maleate/fumarate (based on separate integration of their *CH*(COOEt) signals) present in solution from the total integral of overlapping -O*CH*$_2$CH$_3$ signals of all species present.

(17) Direct addition of 100 equiv (instead of 50 equiv) EDA to a solution of **5** in $CHCl_3$ led to an even lower overall PEA yield of 33% (M_w = 210 kD, M_w/M_n = 4.3).

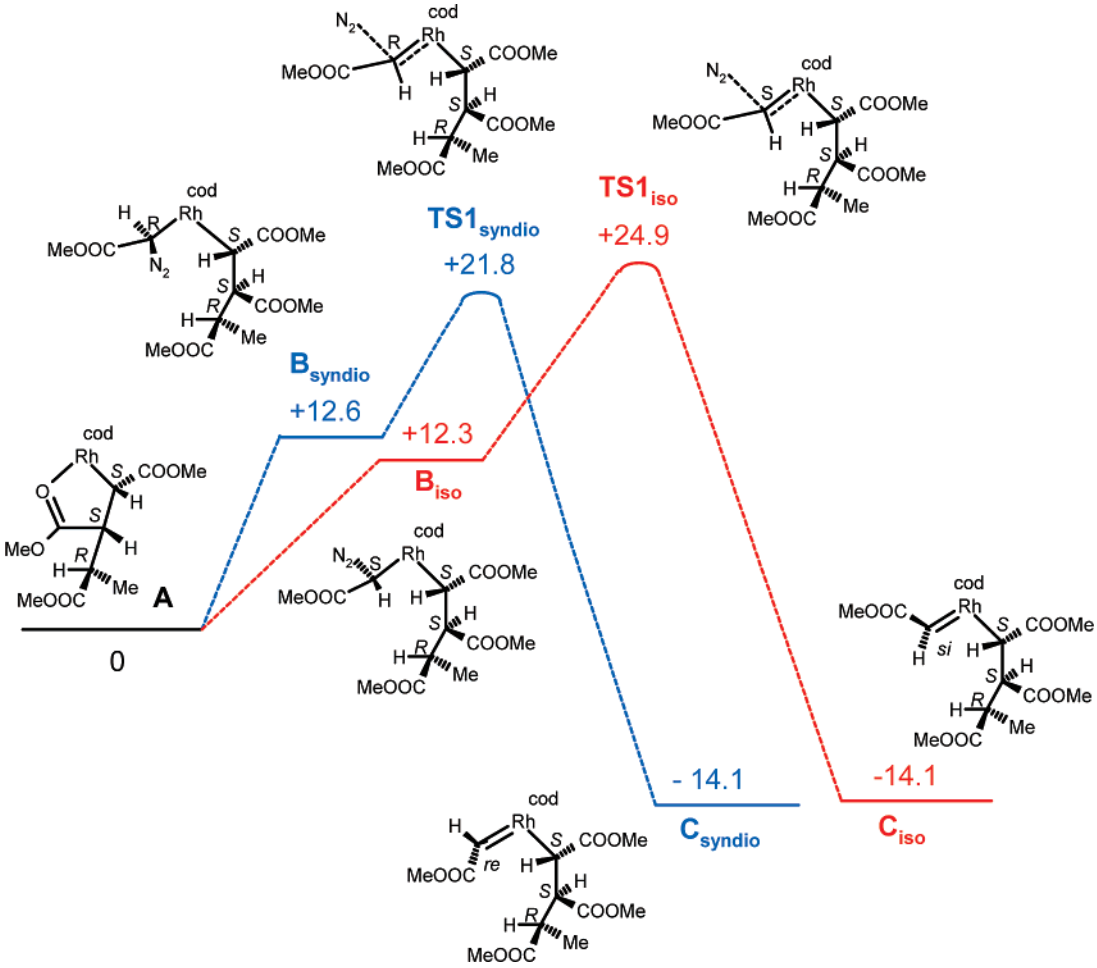

Figure 4. Relative free energies (ΔG^0 in kcal/mol) associated with rate-determining carbene formation steps from **A** and MDA (b3lyp, TZVP), corrected for ZPE and thermal effects (298 K).

reliable chemical shifts for rrrrrr heptads of syndiotactic microstructures are not available for comparison because the probability of racemic propagation P_r is near zero for radical polymerization of dialkyl fumarates. However, observed deviations from expected heptad sequences according to such probability calculations upon polymerization of dimethyl fumarate at higher temperatures have been interpreted in terms of increased amounts of rr triads, giving rise to ^{13}C NMR shifts at ~171 ppm (carbonyl) and ~45.3 ppm (methine). The ^{13}C NMR chemical shifts of the highly stereoregular polymers obtained with Rh and EDA (170.8, 45.4 ppm) are very different from those of the mmmmmm heptads of isotactically enriched poly(dialkyl fumarate)s (170.2, 46.0 ppm), while they correspond to those interpreted as rr triads. On this basis we assign the polymer being *syndiotactic* (Figure 3, see also ref 12).

Computational Studies

The experimental results clearly suggest the involvement of a Rh(diene) active species in chain propagation. This makes the involvement of any Rh^{III} complex (kinetically inert, low affinity for alkenes) rather unlikely, leaving (diene)Rh^{I}(alkyl) as the most plausible active species. Such a species could, for example, be generated in situ by nucleophilic attack of the prolinate oxygen atom on a Rh-bound carbene fragment. On this basis we performed computational studies in search for a plausible mechanistic explanation for the preferred formation of *syndiotactic* polymers with (diene)Rh catalysts.

All calculations were performed with cod as the stabilizing diene and with methyl diazoacetate (MDA) as a smaller model substrate for EDA. Neutral (cod)Rh^{I}{CH(COOMe)}$_3$CH$_3$ species **A** (obtained after three consecutive carbene insertions into a Rh−Me fragment) is probably the smallest possible model that realistically represents the steric and electronic properties of the active catalyst. All calculations were initiated from species **A**, containing a syndiotactic growing chain fragment.[18] As expected, geometry optimization of **A** led to coordination of a carbonyl oxygen atom of the growing chain to the rhodium center. The ester methoxy oxygen atoms can also coordinate to rhodium, but this leads to substantially higher-energy structures, which we therefore did not consider further. The most stable geometry of **A** contains a favorable five-membered ring formed by coordination of the β-carbonyl fragment (see Figure 4). Coordination of the α-carbonyl is also possible, leading to a somewhat higher-energy structure **A′** (+0.7 kcal/mol) which could be considered as a "hetero-allyl" species (see Supporting Information).

Generation of a Rh−carbene fragment requires binding of the prochiral diazo-bearing carbon atom of MDA to Rh after carbonyl dissociation from **A** or **A′**, leading to two possible diastereoisomeric MDA adducts that are close in energy ($\mathbf{B}_{syndio}$ +12.6 kcal/mol; $\mathbf{B}_{iso}$ +12.3 kcal/mol). MDA coordination

(18) This fragment has an *S* configuration of the Rh-bound methine carbon. The methine carbons of the rr triad have *S,S,R* configurations, becoming *R,S,R* after the next carbene insertion.

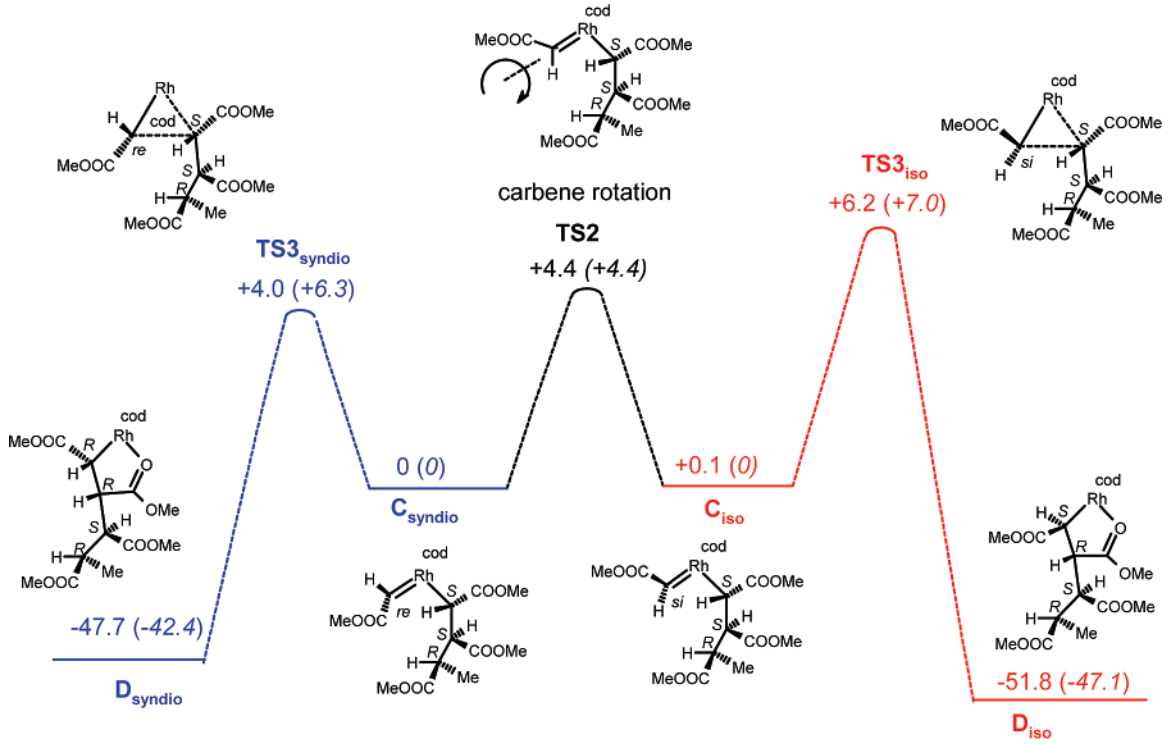

Figure 5. Relative enthalpies ΔH^0 and free energies (ΔG^0 given in between brackets) of isotactic and syndiotactic carbene insertion steps (b3lyp, TZVP) in kcal/mol, corrected for ZPE and thermal effects (298 K).

through a nitrogen atom is also possible (+7.5 kcal/mol) but is not productive[19] and was therefore not considered further.

We failed to find any transition state involving a direct attack of the Rh-bound growing chain on the coordinated MDA fragments in structures **B**. Such a mechanism would lead to structures **D** in a single S_N2-like substitution step, similar to the mechanism recently proposed for BH_3- and Pd-catalyzed oligomerization of EDA.[8,10] It thus seems more likely that our Rh-mediated polymerization reaction proceeds via discrete carbenoid intermediates **C**, and this pathway was further explored.

In good agreement with other computational studies,[20] exothermic formation of the carbenoids **C** seems to proceed via dinitrogen loss from carbon-bound MDA adducts **B**, which is over-all rate limiting along the calculated reaction pathway. The transition-state free energies **TS1** are within a reasonable range for reactions proceeding within hours at RT (Figure 4). The transition state for formation of $\mathbf{C_{syndio}}$ ($\mathbf{TS1_{syndio}}$, +21.8 kcal/mol) lies about 3 kcal/mol lower in free energy than that for formation of $\mathbf{C_{iso}}$ ($\mathbf{TS1_{iso}}$, +24.9 kcal/mol).

Remarkably, the Rh═C bond of structure **C** adopts a parallel orientation with respect to the cod C═C bond *trans* to it. Thus, different d orbitals of the rhodium metal center are used for optimal π backbonding to the carbene fragment and to this C═C bond. As a result, the carbene fragment is pre-organized for migratory insertion into the Rh−C bond of the growing chain, with $\mathbf{C_{syndio}}$ having its *re* face and $\mathbf{C_{iso}}$ having its *si* face oriented for attack of the growing chain. This corresponds to the two possible enantiotopic insertion pathways (*racemic* vs *meso*) leading to syndiotactic and isotactic polymers. For steric reasons, the $\{CH(COOMe)\}_3CH_3$ chains of **B** and **C** adopt approximate *trans-gauche* conformations (torsion angles: C_{Me}−C−C−C ≈ 160° and C−C−C−Rh ≈ 60°). Any other conformation would cause substantial strain, either within the chain itself or between the chain and the Rh(cod) or Rh(carbene) fragments.

Once the carbene fragments are formed, migratory carbene insertion into the Rh−C bonds of **C** to form the insertion products **D** is a strongly exothermic, low-barrier process (Figure 5). Although formation of $\mathbf{C_{syndio}}$ is substantially easier than formation of $\mathbf{C_{iso}}$, carbene rotation provides a relatively low-energy equilibration pathway between these species (**TS2** = +4.4 kcal/mol). The product-forming steps (**C** → **D**) are also calculated to have low activation energies ($\Delta G^{\ddagger}$ = 6.3 and 7.0 kcal/mol), so the final selectivity will not be simply determined by a single limiting step.

It should be noted here that entropy corrections appear to artificially disfavor $\mathbf{TS3_{syndio}}$ relative to $\mathbf{TS3_{iso}}$. The calculated enthalpy difference of 2.2 kcal/mol is reduced to only 0.7 kcal/mol on going to free energies. This is due to contributions from a few very low-frequency modes, for which the harmonic approximation used in the corrections loses its validity. It may be that the use of relative enthalpy values is more appropriate here. Indeed, for smaller models in which we replaced the $-\{CH(COOMe)\}_3CH_3$ growing chain by $-\{CH(COOMe)\}CH_3$ (which is less floppy, thus causing fewer problems associated with low-frequency modes), the free energy for the syndiotactic migratory insertion ($\Delta G^{\ddagger}$ = 3.6 kcal/mol) is 1.5 kcal/mol lower than the corresponding isotactic insertion ($\Delta G^{\ddagger}$ = 5.1 kcal/mol).

In any case, the final selectivity will be intermediate between that expected from **B** → **C** ($k_1/k_{1'}$), as selectivity-determining on the one hand, and rapid $\mathbf{C_{syndio}}$/$\mathbf{C_{iso}}$ equilibration leading to

(19) Howell, J. A. S. *Dalton Trans.* **2007**, 1104.
(20) Cohen, R.; Rybtchinski, B.; Gandelman, M.; Rozenberg, H.; Martin, J. M. L.; Milstein, D. *J. Am. Chem. Soc.* **2003**, *125*, 6532−6546.

Scheme 3. Selectivity of the Syndiotactic over Isotactic Carbene Insertion (k_{syndio}/k_{iso}) Depending on Rate Constants k_1, $k_{1'}$, k_2, $k_{2'}$, k_3, and $k_{3'}$

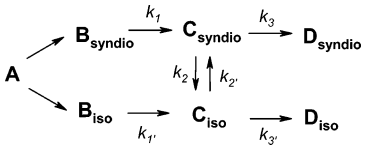

Table 3. Predicted Stereoselectivity k_{syndio}/k_{iso} for a Steady-State Model and Limiting $k_1/k_{1'}$ and $k_3/k_{3'}$ Values Based on Calculated Barriers

	B → C limiting ($k_1/k_{1'}$)	steady-state model	**C → D** limiting ($k_3/k_{3'}$)
$\Delta H^{\ddagger}$	187.8	50.1 (*115.6*[a])	48.6 (*113.2*[a])
$\Delta G^{\ddagger}$	187.8	3.4 (*16.5*[a])	3.4 (*13.0*[a])

[a] Values between brackets based on barriers for **C → *D*** (**TS3$_{syndio}$** and **TS3$_{iso}$**) obtained with smaller, shorter growing chain models (see Supporting Information) keeping **TS1** and **TS2** barriers of the larger model.

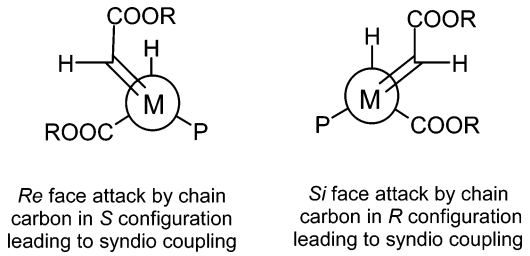

Figure 6. Simplified representation of Rh-mediated "carbene" polymerization under chain-end control, with minimal steric interactions between the substituents of the growing chain and the carbene fragments favoring the **C$_{syndio}$ → D** migratory insertion.

C → D ($k_3/k_{3'}$), as selectivity-determining on the other hand (see Scheme 3).

Table 3 lists the actual predicted selectivity (from a steady-state model, see Supporting Information) and these limiting values, based on both enthalpy and free-energy differences. Regardless of the energies used, syndiotactic propagation is seen to be preferred. However, all of the energy differences here are rather small, close to the error limits of the computational methods employed, and the differences should be treated with caution. In particular, the balance between rotation and insertion, which has a significant effect on predicted stereoselectivity, can also be expected to have a relatively large error margin.

The interplay between the different rates implies that the ancillary ligand could well influence the stereoselectivity. Ancillary ligand effects are difficult to predict though. For cod, competition between the two respective carbene-forming steps (**B → C**) and the two respective carbene insertion steps (**C → D**) is clearly determined by carbene−chain end interactions (for a simplified representation, see Figure 6), but this could easily change with other (diene) ligands. Electronic and steric properties of the ancillary ligand (e.g., the bite-angles) could have an influence on the absolute *and* relative carbene formation and insertion barriers. The ancillary ligand could also affect the carbene rotation barrier, which depends on the π-acceptor strength of the diolefin as well as its steric properties. Variation of the rotation barrier would shift the selectivity between the **B → C** and **C → D** limiting values in Table 3.

A selection of changes in bond lengths and angles associated with carbene formation (N_2 loss from MDA adduct **B** via **TS1** to carbenoid **C**) and migratory insertion (from **C** to **TS3**) is

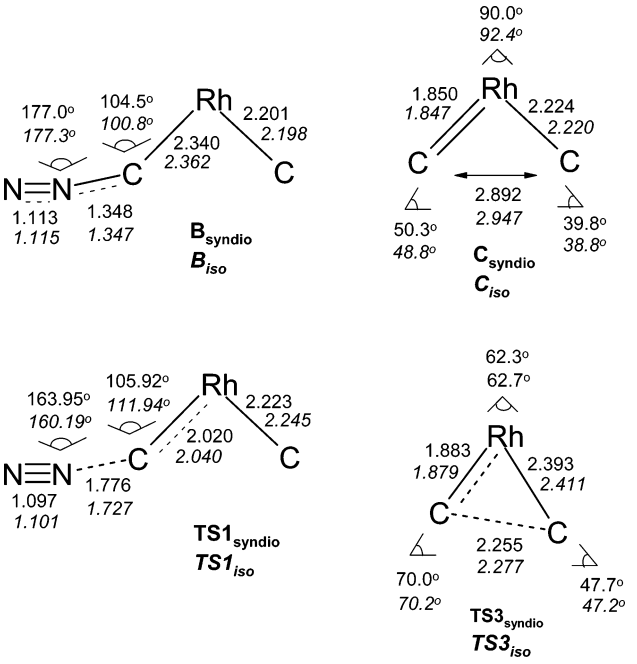

Figure 7. Selection of bond lengths (Å) and angles (deg) associated with carbene formation and migratory insertion for both the calculated isotactic and syndiotactic pathways.

shown in Figure 7. The geometric differences between the syndio and iso paths are clearly minor and support our interpretation of weak steric monomer−chain end interactions as the selectivity-determining factor when applying cod as the ancillary ligand.[21]

Conclusions

[(*N*,*O*-ligand)Rh(diene)] complexes mediate formation of high-molecular weight and highly stereoregular functionalized polymethylenes (PEA) from ethyl diazoacetate (EDA). On the basis of a comparison of the ^{13}C NMR data with those obtained for isotactic enriched polyfumarates, the polymers obtained with Rh and EDA are found to be syndiotactic. Variation of the anionic *N*,*O*-ligand is only of influence on the polymer yields and not on the polymer properties, whereas variation of the diene ligand has a marked influence on the polymer properties. This suggests that the *N*,*O*-ligand is only involved in the *initiation* while the diene ligand is the metal-supporting ligand of the catalytically active species during the *propagation* steps.

Kinetic studies indicate that only a small fraction of the Rh (1−5%) is involved in polymerization catalysis; the linear relation between polymer yield and M_w suggests that the chains terminate slowly and chain transfer is not observed. Oligomers and fumarate/maleate byproducts are most likely formed from other "active" species.

DFT calculations suggest a chain-growth pathway involving consecutive migratory insertion steps of carbene fragments, formed from the carbon-bound diazo substrate by rate-limiting dinitrogen loss, into the Rh−C bond of the growing chain. The

(21) The computational results are in *agreement* with stereoregulation under chain-end control, but do not strictly exclude the possibility of other contributing factors such as, for example, higher-order (helical) growing chain structures influencing the stereo-electronic environment around the active site. Additional studies are required for a fully quantitative understanding, taking into account the influence of all possible stereo-errors on the carbene formation and carbene insertion steps, using COOEt groups instead of COOMe model fragments in the calculations.

Table 4. Tabulated ^{1}H NMR Chemical Shift Values (δ in ppm) of Compounds **6** and **7**

	[(dcp)Rh(pro)] (**7**) 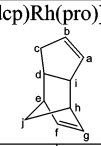				[(nbd)Rh(pro)] (**6**) 
proton	**7a**	**7a'**	**7b**	**7b'**	-
a	4.81	4.04	4.92	4.52	-
b	4.92	4.04	4.98	4.04	-
c	2.28, 2.25, 2.21 and 1.85-1.77				-
d	2.42, 2.36 and 2.31				-
e					3.90
f	3.81	4.67	4.04	4.70	4.02 and 3.98
g	5.50	6.39	5.18	6.20	4.02 and 3.98
h	3.33	3.29	3.29	3.29	-
i	3.05				-
j	2.18-1.88 and 1.75-1.71				1.25
NH	4.43 and 4.22-4.16				-
COO-CH	3.76 and 3.69				3.70
NH-CH_2	3.24, 3.12, 2.99, 2.86, 2.67 and 2.62				2.86-2.73
CH_2-CH-COO	2.18-1.88				2.19-2.12 and 2.05-1.91
NH-CH_2-CH_2	1.85-1.77 and 1.67-1.53				2.05-1.91 and 1.69-1.61

computational results explain the formation of syndiotactic polymers via chain-end control,[21] modulated by carbene rotation. These new insights provide new tools for catalyst optimization to further improve this novel polymerization reaction.

Experimental Section

General Procedures. All manipulations were performed under an argon atmosphere using standard Schlenk techniques. Methanol and dichloromethane distilled from calcium hydride and toluene distilled from sodium were used for metal complex synthesis. [{Rh^{I}(1,5-cyclooctadiene)(μ-OAc)}]$_2$ (**1**),[22] [{Rh^{I}(2,5-norbornadiene)(μ-Cl)}]$_2$,[23] and [{Rh^{I}(*endo*-dicyclopentadiene)(μ-Cl)}]$_2$[24] were prepared according to literature procedures. The syntheses and catalytic activity of [(picolinate)Rh^{I}(1,5-cyclooctadiene] (**3**), [(quinolinate)Rh^{I}(1,5-cyclooctadiene)] (**4**), and [(L-prolinate)Rh^{I}(1,5-cyclooctadiene)] (**5**), have been reported previously.[12] All other chemicals were purchased from commercial suppliers and used without further purification. NMR spectroscopy experiments were carried out on a Varian Inova 500 spectrometer (500 and 125 MHz for ^{1}H and ^{13}C, respectively) or a Varian Mercury 300 spectrometer (300 and 75 MHz for ^{1}H and ^{13}C, respectively). Assignment of the signals was aided by COSY, NOESY, ^{13}C HSQC, and APT experiments. Solvent shift reference for ^{1}H NMR spectroscopy: $CDCl_3$: $\delta_H = 7.26$, DMSO-d_6: $\delta_H = 2.50$. For ^{13}C NMR spectroscopy: $CDCl_3$: $\delta_C = 77.0$, DMSO-d_6: $\delta_C = 39.43$. Abbreviations used are: s = singlet, d = doublet, dd = doublet of doublets, t = triplet, q = quartet, m = multiplet, br = broad, cod = 1,5-cyclooctadiene, gly = glycinate, nbd = 2,5-norbornadiene, dcp = dicyclopentadiene, pro = prolinate. Elemental analyses (CHN) were performed by the Kolbe analytical laboratory in Mülheim an der Ruhr (Germany).

[(Glycinate)Rh^{I}(1,5-cyclooctadiene)] (2). A solution of [{Rh^{I}(1,5-cyclooctadiene)(μ-OAc)}]$_2$ (**1**) (200 mg, 0.4 mmol) in toluene (10 mL) was added to a suspension of glycine (56 mg, 0.7 mmol) in methanol (6 mL). The yellow solution was stirred at room temperature for 20 h. Subsequently, volatiles were evaporated, resulting in a yellow solid. The product was recrystallized from hot methanol, affording yellow crystals (76 mg, 0.3 mmol, 38%).

^{1}H NMR (300 MHz, DMSO-d_6, 292 K): δ 3.97 (t, $^3J_{HH} = 6.5$ Hz, 2H, NH_2), 3.90 (br s, 4H, cod-CH), 3.03 (t, $^3J_{HH} = 6.5$ Hz, 2H, CH_2-COO), 2.32 (m, 4H, cod-CH_2), 1.71 (dd, $^3J_{HH} = 7.5$ Hz, 4H, cod-CH_2). ^{13}C NMR (75 MHz, DMSO-d_6, 292 K): δ 182.3 (COO), 77 (br, cod-CH), 45.8 (gly-CH_2), 30.1 (cod-CH_2). Elemental analysis for $C_{10}H_{16}NO_2Rh$: calcd C 42.12, H 5.66, N 4.91; found C 41.98, H 5.62, N 4.83.

[(L-Prolinate)Rh^{I}(2,5-norbornadiene)] (6). A solution of proline (125 mg, 1 mmol) and sodium hydroxide (43 mg, 1 mmol) in methanol (5 mL) was added to a brown suspension of [{Rh^{I}(2,5-norbornadiene)(μ-Cl)}]$_2$ (250 mg, 0.5 mmol) in methanol (5 mL). The obtained clear-brown solution was stirred for 1 h at room temperature. The solvent was removed in vacuo, and the product was dissolved in dichloromethane (15 mL). The mixture was filtrated, and subsequently the solvent was evaporated. The product was obtained as a yellow powder (264 mg, 0.8 mmol, 80%).

^{1}H NMR (500 MHz, $CDCl_3$, 298 K): δ 4.02, 3.98 (br s, 4H, nbd-CH olefinic), 3.90 (s, 2H, nbd-CH), 3.70 (m, 1H, C*H*-COO), 2.86−2.73 (m, 2H, CH_2-NH), 2.19−2.12 (m, 1H, CH_2-CH), 2.05−1.91 (m, 2H, CH_2-CH_2-CH-COO), 1.69−1.61 (m, 1H, CH_2-CH_2-CH), 1.25 (s, 2H, nbd-CH_2). ^{13}C NMR (125 MHz, $CDCl_3$, 298 K): δ 184.99 (COO), 62.51 (COO-*C*H), 61.69 (nbd-CH_2), 51.02 (nbd-CH non-olefinic), 49.13 (NH-CH_2), 30.13 (COO-CH-*C*H_2), 25.72 (NH-CH_2-*C*H_2) (olefinic carbon signal is probably too broad to be observed). Elemental analysis for $C_{12}H_{16}NO_2Rh\cdot 0.2CH_2Cl_2$: calcd C 44.54, H 5.04, N 4.24; found C 44.79, H 5.13, N 4.37. NMR reveals inclusion of ~0.2 equiv of CH_2Cl_2 in the crystal lattice.

[(L-Prolinate)Rh^{I}(*endo*-dicyclopentadiene)] (7). A solution of proline (115 mg, 1 mmol) and sodium hydroxide (40 mg, 1 mmol) in methanol (5 mL) was added to a suspension of [{Rh^{I}(*endo*-dicyclopentadiene)(μ-Cl)}]$_2$ (270 mg, 0.5 mmol) in methanol (5 mL). The obtained clear orange-brown solution was stirred for 1 h at room temperature. The solvent was removed in vacuo, and the product was dissolved in dichloromethane (20 mL). The mixture was filtrated, and subsequently the solvent was evaporated. The product was obtained as an orange-yellow powder (244 mg, 0.6 mmol, 65%).

^{1}H NMR (500 MHz, $CDCl_3$, 298 K) (mixture of four isomers: **7a**, **7a′**, **7b**, and **7b′**): δ 6.39 (s, 1H, C_gH of **7a′**), 6.18 (s, 1H, C_gH of **7a′**), 5.50 (s, 1H, C_gH of **7a**), 5.18 (s, 1H, C_gH of **7b**), 4.98 (s, 1H, C_bH of **7b**), 4.92 (overlapping s, 2H, C_bH of **7a** and C_aH of **7b**), 4.81 (s, 1H, C_aH of **7a**), 4.70 (s, 1H, C_fH of **7b′**), 4.67 (s, 1H, C_fH of **7a′**), 4.52 (s, 1H, C_aH of **7b′**), 4.43 (m, 1H, NH), 4.22−4.16 (m, 3H, NH), 4.04 (overlapping s, 4H, C_aH, and C_bH of **7a′**, C_bH of **7b′**, and C_fH of **7b**), 3.81 (s, 1H, C_fH of **7a**), 3.76, 3.69 (2× m, 4H, COO-CH), 3.33 (s, 1H, C_hH of **7a**), 3.29 (overlapping s, 3H, C_hH of **7a′**, **7b**, and **7b′**), 3.05 (overlapping s, 4H, 4× C_iH), 3.24, 3.12, 2.99, 2.86, 2.67, 2.62 (6× m,

(22) Sheldrick, W. S.; Günther, B. *J. Organomet. Chem.* **1989**, *375*, 233−243.
(23) (a) Chatt, J.; Venanzi, L. M. *J. Chem. Soc.* **1957**, 4735. (b) Abel, E. W.; Bennett, M. A.; Wilkinson, G. *J. Chem. Soc.* **1959**, 3178.
(24) Saeed, I.; Shiotsuki, M.; Masuda, T. *Macromolecules* **2006**, *39*, 8977.

Table 5. Tabulated ^{13}C NMR Chemical Shift Values (δ in ppm) of Compounds **6** and **7**

	[(dcp)Rh(pro)] (**7**) 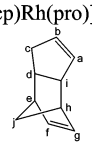				[(nbd)Rh(pro)] (**6**) 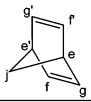
carbon	**7a**	**7a'**	**7b**	**7b'**	-
a	87.59	78.48	87.08	78.48	-
b	85.22	73.59	84.18	73.22	-
c	34.84, 34.73, 34.60 and 34.39				-
d	44.82, 44.54, 44.48, 44.42, 44.35 and 44.24				-
e					51.02
f	64.84	75.94	65.78	75.14	-
g	89.59	102.28	90.52	101.82	-
h	56.91, 56.48, 56.12, 55.61, 55.18, 54.33 and				-
i	54.15				-
j	59.81, 59.52 and 59.35				61.69
COO	184.65, 184.33 and 183.86				184.99
COO-*C*H	63.77, 63.47 and 63.41				62.51
NH-CH_2	49.64, 49.42 and 48.93				49.13
CH_2-CH-COO	30.23, 29.89 and 29.62				30.13
NH-CH_2-*C*H_2	25.35, 25.02, 24.98 and 24.82				25.72

8H, NH-C*H*$_2$), 2.42, 2.36, 2.31 (overlapping s, C_dH and C_eH), 2.28, 2.25, 2.21 (3× s, C_cH$_2$), 2.18−1.88 (overlapping m, C_jH$_2$ and COO-CH-C*H*$_2$), 1.85−1.77 (m, C_cH$_2$ and COO-CH-CH$_2$-C*H*$_2$), 1.75−1.71 (m, C_jH$_2$), 1.67−1.53 (COO-CH-CH$_2$-C*H*$_2$). ^{13}C NMR (125 MHz, $CDCl_3$, 298 K): δ 184.65, 184.33, 183.86 (3× s, COO), 102.28 (d, $^1J_{Rh-C}$ = 12 Hz, C_gH of **7a′**), 101.82 (br s, C_gH of **7b′**), 90.52 (d, $^1J_{Rh-C}$ = 13 Hz, C_gH of **7b**), 89.59 (d, $^1J_{Rh-C}$ = 13 Hz, C_gH of **7a**), 87.59 (d, $^1J_{Rh-C}$ = 11 Hz, C_aH of **7a**), 87.08 (d, $^1J_{Rh-C}$ = 15 Hz, C_aH of **7b**), 85.22 (d, $^1J_{Rh-C}$ = 11 Hz, C_bH of **7a**), 84.18 (d, $^1J_{Rh-C}$ = 11 Hz, C_bH of **7b**), 78.48 (d, $^1J_{Rh-C}$ = 12 Hz, C_aH of **7a′** and **7b′**), 75.94 (d, $^1J_{Rh-C}$ = 14 Hz, C_fH of **7a′**), 75.14 (br s, C_fH of **7b′**), 73.59 (d, $^1J_{Rh-C}$ = 13 Hz, C_bH of **7a′**), 73.22 (br s, C_bH of **7b′**), 65.78 (d, $^1J_{Rh-C}$ = 16 Hz, C_fH of **7b**), 64.84 (d, $^1J_{Rh-C}$ = 16 Hz, C_fH of **7a**), 63.77, 63.47, 63.41 (3× s, COO-*C*H), 59.81, 59.52, 59.35 (3× s, C_jH$_2$), 56.91 (br s), 56.48, 56.12, 55.61, 55.18, 54.33, 54.15 (br s) (7× s, C_hH and C_iH), 49.64, 49.42, 48.93 (3× s, NH-CH_2), 44.82, 44.54, 44.48, 44.42, 44.35, 44.24 (6× s, C_dH and C_eH), 34.84, 34.73, 34.60, 34.39 (br) (4× s, C_cH$_2$), 30.23, 29.89, 29.62 (3× s, COO-CH-*C*H$_2$), 25.35, 25.02, 24.98, 24.82 (br) (4× s, COO-CH-CH$_2$-*C*H$_2$). Elemental analysis for $C_{15}H_{20}NO_2$-Rh·0.25CH_2Cl_2: calcd C 48.80, H 5.52, N 3.71; found C 48.81, H 5.57, N 3.74. NMR reveals inclusion of ~0.25 equiv of CH_2Cl_2 in the crystal lattice (Tables 4 and 5).

Polymerization of Carbenes from EDA to Poly(ethyl 2-ylidene-acetate). Ethyl diazoacetate (EDA) (2 mmol) was added to a yellow solution of catalyst precursor (0.02 mmol of **1** and 0.04 mmol of **2**−**7**) in chloroform (5 mL) (**2** dissolved after addition of EDA). Upon addition, gas evolution was visible, and the color of the reaction mixture became slightly darker. The mixture was stirred for 14 h at room temperature. Subsequently the solvent was removed in vacuo, and methanol was added to the oily residue. The precipitate was centrifuged and washed with methanol until the washings were colorless. The resulting white powder was dried in vacuo and identified as poly(ethyl 2-ylidene-acetate) (PEA) using ^1H NMR spectroscopy (spectroscopic data of the polymer have been reported previously).[12]

Experiments in which the polymerization was followed in time were performed using identical conditions (^1H NMR: 300 MHz, $CDCl_3$, 292 K).

Polymer and Oligomer Characterization. Molecular mass distributions were measured using size exclusion chromatography (SEC) on a Shimadzu LC-20AD system with Waters Styragel HR1, HR2, and HR4 columns in series and a Shimadzu RID-10A refractive index detector, using dichloromethane as mobile phase at 1 mL/min and T = 40 °C. Polystyrene standards in the range of 760−1880000 g/mol (Aldrich) were used for calibration. Previously, SEC-MALLS experiments showed that the values obtained by calibration against polystyrene standards slightly underestimate the molecular weights (M_w) and somewhat overestimate the polydispersities (M_w/M_n) of poly(ethyl 2-ylidene-acetate).[12]

DFT Calculations. The geometry optimizations were carried out with the Turbomole program[25a,b] coupled to the PQS Baker optimizer.[26] Geometries were fully optimized as minima or transition states at the b3-lyp level[27] using the polarized triple-ξ TZVP basis[25c,f] (small-core pseudopotential[25c,e] on Rh or Ir). All stationary points were characterized by vibrational analysis (numerical frequencies); ZPE and thermal corrections (entropy *and* enthalpy, 298 K, 1 bar) from these analysis are included. Energies are reported both as enthalpies and free energies (Table S1). Optimized geometries, visualized with the PLATON[28] program (rendered with POVRAY), are shown in Figures S2−S21 in the Supporting Information.

Acknowledgment. This work was supported by the Netherlands Organization for Scientific Research (NWO-CW), the University of Amsterdam, and the Canada Foundation for Innovation (CFI Project 10831). We thank Prof. P. W. N. M. van Leeuwen, T. G. Bloemberg, and J. Flapper for helpful discussions and J. A. J. Geenevasen for his assistance with the NMR measurements.

(25) (a) Ahlrichs, R; et al. *Turbomole Version 5*, January 2002. Theoretical Chemistry Group, University of Karlsruhe. (b) Treutler, O.; Ahlrichs, R. *J. Chem. Phys.* **1995**, *102*, 346−354. (c) Turbomole basis-set library; *Turbomole, Version 5*, see ref 25a. (d) Schäfer, A.; Horn, H.; Ahlrichs, R. *J. Chem. Phys.* **1992**, *97*, 2571−2577. (e) Andrae, D.; Haeussermann, U.; Dolg, M.; Stoll, H.; Preuss, H. *Theor. Chim. Acta* **1990**, *77*, 123−141. (f) Schäfer, A.; Huber, C.; Ahlrichs, R. *J. Chem. Phys.* **1994**, *100*, 5829−5835. (g) Ahlrichs, R.; May, K. *Chem. Phys.* **2000**, *2*, 943.

(26) (a) PQS version 2.4; Parallel Quantum Solutions: Fayetteville, Arkansas, U.S.A., 2001 (the Baker optimizer is available separately from PQS upon request). (b) Baker, J. *J. Comput. Chem.* **1986**, *7*, 385−395.

(27) (a) Lee, C.; Yang, W.; Parr, R. G. *Phys. Rev. B* **1988**, *37*, 785−789. (b) Becke, A. D. *J. Chem. Phys.* **1993**, *98*, 1372−1377. (c) Becke, A. D. *J. Chem. Phys.* **1993**, *98*, 5648−5652. (d) Calculations were performed using the Turbomole functional "b3-lyp", which is not identical to the Gaussian "B3LYP" functional.

(28) Spek, A. L. *PLATON*. A Multipurpose Crystallographic Tool; Utrecht University: Utrecht, The Netherlands, 2003.

Supporting Information Available: ^{1}H NMR spectrum of the poorly defined oligomers, energy profile for the carbene rotation, details concerning the calculation of the syndio/iso insertion preference, energies and optimized geometries of the minima and transitions states and complete ref 25a; zip file containing PDB and XYZ files. This material is available free of charge via the Internet at http://pubs.acs.org.

JA073897+